Analyst

PAPER

View Article Online
View Journal | View Issue

Cite this: *Analyst*, 2015, **140**, 4642

A sensitive biosensor with a DNAzyme for lead(II) detection based on fluorescence turn-on†

Yang Guo, Junting Li, Xiaoqian Zhang and Yanli Tang*

Received 8th April 2015,
Accepted 29th April 2015

DOI: 10.1039/c5an00677e

www.rsc.org/analyst

In this paper, we described a new DNAzyme-based fluorescent biosensor for the detection of Pb^{2+}. In the biosensor, the bulged structure is formed between the substrate labeled with fluorescein amidite (FAM) and DNAzyme after being annealed. Ethidium bromide (EB), the DNA intercalator, then intercalates into the double-stranded DNA section. Once FAM is excited, the FRET takes place from FAM to EB, which leads to the fluorescence of FAM decreasing greatly. In the presence of Pb^{2+}, the substrate is cleaved by DNAzyme, which breaks the bulged structure. Then EB is released and the FRET from FAM to EB is inhibited. In this case, the fluorescence of FAM increases dramatically. Thus, the Pb^{2+} ions can be detected by measuring the fluorescence enhancement of FAM. Under optimal conditions, the increased fluorescence intensity ratio of FAM is dependent on the lead level in the sample, and exhibits a linear response over a Pb^{2+} concentration range of 0–100 nM with a detection limit of 530 pM. The sensor showed high selectivity in the presence of a number of interference ions. The river water samples were also tested with satisfying results by using the new method. This sensor is highly sensitive and simple without any additional treatments, which provides a platform for other biosensors based on DNAzyme.

Introduction

Heavy metals are widespread environmental pollutants, and most of them are toxic to human health such as lead ions (Pb^{2+}).[1] Pb^{2+} could cause serious damage to the brain and central nervous system even at low concentrations, leading to fatigue, headaches, irreversible learning difficulties, lung tumors, and illnesses.[2,3] According to the Environmental Protection Agency (EPA), 15 ppb (0.07 μM) of lead is the safety limit in drinking water,[4] while the International Agency for Research on Cancer (IARC) has a lower threshold of 10 ppb (48.26 nM) in food and water. Therefore, the development of simple, rapid and sensitive sensors plays an important role in detection of lead ions in environmental and biological samples.

Traditional methods for detection of heavy metals have been developed for many years, including atomic adsorption spectrometry, inductively-coupled plasma mass spectrometry, inductively-coupled plasma atomic emission spectrometry, voltammetric detection and UV vis spectrometry.[5–7] These methods present good sensitivity for lead, however most of them require time-consuming pretreatment procedures and expensive instruments, which limit their on-site and real-time detection. A lot of methods thus have been developed for metal assay in order to provide on-site analysis.[8–13] Notably, fluorescent platforms for lead detection have attracted much attention because they have facile operation and high sensitivity, cause less cell-damage, and have the ability to provide real-time information.[14–16]

Very recently, Zhang and Zhu published a critical review on the development of functional nucleic acid-based sensors for the detection of heavy metal ions.[17] DNAzyme as a sensor platform for detection of lead ions has been studied extensively for several years[17,18] and many of the DNAzyme-based sensors required using advanced materials including quantum dots,[19] gold nanoparticles,[20–24] graphene,[25,26] *etc.* In addition, some methods based on phosphorothioate modification,[27] strand displacement amplification reaction,[28] rolling circle amplification or exonuclease aided recycling amplification[24,29,30] provide high sensitivity, however limitations still exist, such as needing complicated and long-time operation.

Herein, we developed a fluorescence turn-on method for sensitive and selective detection of Pb^{2+} based on 17E DNAzyme and the cleavage substrate 17S labeled with FAM.[31] In this method, ethidium bromide (EB), a double-stranded DNA intercalator, is used as an energy acceptor in the fluorescence resonance energy transfer (FRET) process, leading to the fluorescence of FAM decreasing. First, 17E and 17S-FAM

Key Laboratory of Applied Surface and Colloid Chemistry, Ministry of Education, Key Laboratory of Analytical Chemistry for Life Science of Shaanxi Province, School of Chemistry and Chemical Engineering, Shaanxi Normal University, Xi'an 710062, P. R. China. E-mail: yltang@snnu.edu.cn; Fax: (+086) 029-81530727; Tel: (+086) 029-81530844

†Electronic supplementary information (ESI) available. See DOI: 10.1039/c5an00677e

form a bulged structure after hybridization. EB then intercalates into the double-stranded DNA section. When the solution is excited at 490 nm, the FRET occurs from FAM to EB, which leads to the fluorescence intensity of FAM decreasing greatly.[32–34] In the presence of lead ions, the substance 17S-FAM is cleaved by 17E DNAzyme, resulting in the FRET being broken. The fluorescence intensity of FAM thus increases dramatically. This fluorescence turn-on method exhibits excellent selectivity and sensitivity. Furthermore, this simple and rapid technique could provide a new platform for DNAzyme-based sensors.

Experimental

Reagents and instruments

Materials and measurements. The oligonucleotides were purchased from Takara. HEPES-Na, ethidium bromide (EB) and other chemicals were purchased from Shanghai Sangon Biological Engineering Technology Co. Ltd. Lead(II) acetate trihydrate was purchased from Sinopharm Chemical Reagent Co. Ltd. The oligonucleotide sequences used in our experiments are as follows: 17S-FAM, 5′-FAM-$(CH_2)_6$-ACT CAC TAT rAG GAA GAG ATG; 17E, 5′-CAT CTC TTC TCC GAG CCG GTC GAA ATA GTG AGT.[31] The oligonucleotide 17S-FAM could form a specific bulged structure with 17E. The concentrations of all oligonucleotides were determined by measuring the absorbance spectra at 260 nm using a PekinElmer Lambda 35 spectrophotometer. The fluorescence spectra were recorded on a Hitachi F-7000 spectrophotometer equipped with a xenon excitation source. All solutions were prepared with ultrapure water purified using a Millipore filtration system.

Condition optimization. In 2.0 mL HEPES-Na buffer (100 mM) at pH 7.2, 20 nM (strand concentration) 17S-FAM and 20 nM 17E were incubated for 5 min at room temperature. Then, 1 μM EB was added and incubated for 3 min. The fluorescence emission spectrum was measured with the excitation wavelength of 490 nm. The measurement of fluorescence spectra at different concentrations of EB (2 μM, 3 μM, 4 μM and 5 μM) was done according to the same process.

Pb^{2+} assay. 20 nM 17S-FAM and 20 nM 17E were incubated in 100 mM HEPES-Na buffer at pH 7.2 for 5 min at room temperature. Then, the solution was treated with an aliquot of Pb^{2+} (1–400 mol L^{-1}) for 20 min at room temperature. After incubation, ethidium bromide (EB) was added into the solution, and the fluorescence spectra of these samples were recorded on a Hitachi F-7000 fluorescence spectrophotometer with the excitation wavelength of 490 nm.

Assay for Pb^{2+} as a function of incubating time. The catalytic strand 17E (20 nM) was incubated with the substrate strand 17S-FAM (20 nM) to form a 17E-17S-FAM duplex in HEPES-Na buffer (100 mM, 2 mL, pH 7.3) at room temperature for 5 min. The solution of the 17E-17S-FAM duplex (4.0×10^{-8} M) was treated with Pb^{2+} at room temperature (400 nM) for 0, 5, 10, 15, 20, and 25 min, respectively. After incubation, EB (4 μM) was added. The fluorescence spectra of these samples were recorded on a Hitachi F-7000 fluorescence spectrophotometer with the excitation wavelength of 490 nm. The fluorescence spectra measurements after certain incubation time at different concentrations of Pb^{2+} (10, 100, and 200 nM) were carried out according to the same process.

Selectivity assay. To verify the specificity of Pb^{2+} to DNAzyme, we used Mg^{2+}, Mn^{2+}, K^+, Ni^{2+}, Cd^{2+}, Ca^{2+}, Cu^{2+}, Hg^{2+}, Na^+, Zn^{2+}, Co^{2+} and their mixture to replace Pb^{2+} to react with a 17E-17S-FAM duplex. According to the afore-mentioned experimental procedure, the fluorescence spectra were measured under the same conditions.

Real sample assay. River water samples were collected from Xi'an, Shaanxi province, PR China. The concentrations of lead in these samples were detected by the above-mentioned procedures.

Results and discussion

As shown in Scheme 1, 17E DNAzyme was first hybridized with its substrate 17S-FAM to form the 17E-17S-FAM duplex. When FAM is excited, the strong green fluorescence was observed at 520 nm. It is well-known that ethidium bromide can intercalate within the grooves of double-stranded DNA (dsDNA).[32] After the addition of EB, EB intercalates within the dsDNA section among the 17E-17S-FAM duplexes, then the FRET from FAM to EB occurs upon excitation of FAM at 490 nM because of the desirable spectral overlap between FAM emission and EB absorption (Fig. S1 in the ESI†).[33,34] Meanwhile, the fluorescence of FAM decreases greatly. In this case, EB functions as an energy acceptor to decrease the FAM signal intensity. Compared to the fluorescence quencher-labelled method,[35] this assay frees the quencher from labelling on the ends of nucleotides, which makes the detection simpler and cost-effective. Upon the addition of Pb^{2+} in the test solution, the DNAzyme is activated and then the substrate strand is hydrolyzed into two parts at the cleavage site (rA), which leads to the fluorescein-labeled substrate strand and the DNAzyme strands

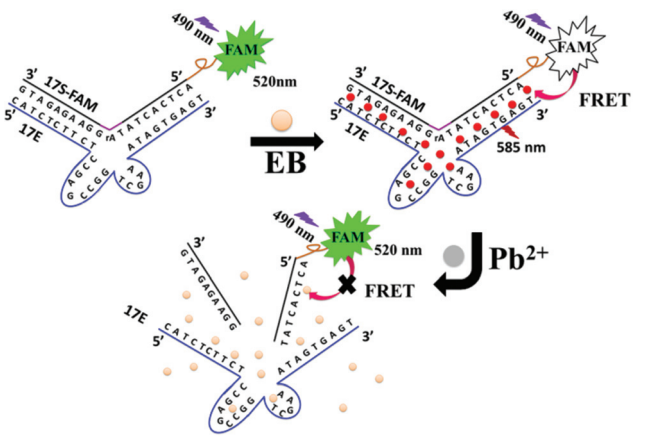

Scheme 1 The proposed principle of Pb^{2+} sensing.

are separated.[35] In this case, EB is released from dsDNA and stays away from FAM, which blocks the FRET from FAM to EB when FAM is excited at 490 nM. Accordingly, the fluorescence of FAM increases. Therefore, the fluorescence signal recovery makes it possible to detect Pb^{2+} by fluorescence spectroscopy.

Fig. 1 shows the fluorescence emission spectra of 17E-17S-FAM duplex/EB in the absence/presence of Pb^{2+}. The 17E-17S-FAM duplex (20 nM) emits strong fluorescence when it is excited at 490 nm. The concentration of EB was optimized by detecting the FRET ratio from FAM to EB when the concentration of the 17E-17S-FAM duplex was fixed at 20 nM. As shown in Fig. S2 (ESI†), when the concentration of EB is 4 μM, the FRET ratio reaches the plateau. Therefore, a 20 nM 17E-17S-FAM duplex and 4 μM EB were selected for the following analytical purposes. Possibly due to the 17E-17S-FAM forming a bulge structure, the unfavourable chain length and orientations result in the relative low fluorescence emission of EB. However, the FAM fluorescence intensity still can be quenched dramatically by FRET. As shown in Fig. 1, in the solution of a 17E-17S-FAM duplex, EB was added and then the fluorescence spectrum was recorded. Because the EB can intercalate into the dsDNA, it is unquestionable that the FRET is observed from FAM to EB when FAM is excited. Accordingly, the fluorescence intensity of FAM decreases dramatically. In the presence of Pb^{2+}, the 17S-FAM substrate is cleaved by Pb^{2+} resulting in the release of EB. Therefore, the FRET is inhibited because of the long distance between FAM and EB, leading to the great enhancement of FAM fluorescence intensity that is the same as the 17E-17S-FAM duplex without EB. Thus, a simple and sensitive fluorescence turn-on platform is set up to detect Pb^{2+}.

As shown in Fig. 2, the fluorescence spectra of 17E-17S-FAM duplex/EB were recorded at different concentrations of Pb^{2+} from 0 to 400 nM. When the concentration of lead ions increases, the fluorescence intensity of FAM increases from around 620 to 6930 because of more and more 17E-17S-FAM duplexes being hydrolyzed by lead ions. Fig. S3† shows the increased fluorescence intensity ratio of FAM ($I/I_0 - 1$) at 520 nm which is dependent on the lead ion concentration. At the range of 0–150 nM, the ratio $I/I_0 - 1$ increases dramatically with the increasing concentration of lead ions. When the concentration of lead ions was added to above 150 nM, the ratio still increases but the change is not obvious. When the concentration of lead ions is greater than 300 nM, the fluorescence intensity isn't enhanced further and a plateau is reached. As shown in Fig. 2b, at the low concentration of lead ions with a range from 0 to 100 nM, the increased ratio is linearly dependent on the concentration of lead ions. The fitting equation is $y = 0.00655 + 0.03605x$ ($R^2 = 0.998$). Thus, the detection limit of 530 pM was obtained reasonably, which is lower than most of that reported previously by Li *et al.*[36]

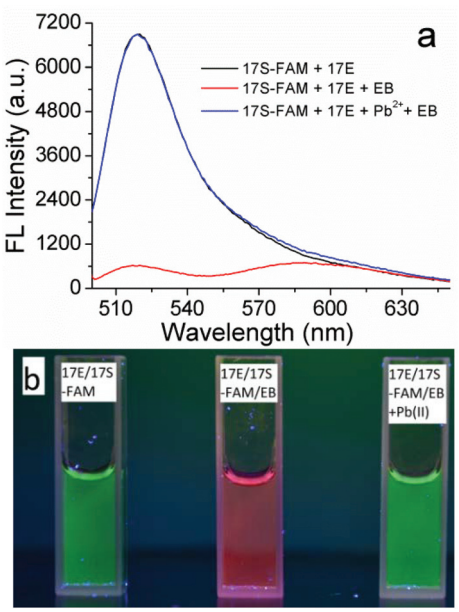

Fig. 1 (a) Fluorescence spectra of 17E/17S-FAM/EB in the absence and presence of lead ions. [17S-FAM] = 2×10^{-8} M, [17E] = 2×10^{-8} M, [EB] = 4×10^{-6} M, [Pb^{2+}] = 300 nM. The excitation wavelength is 490 nM. (b) Fluorescence photographs of 17E/17S-FAM/EB in the absence and presence of lead ions. [17S-FAM] = 2×10^{-7} M, [17E] = 2×10^{-7} M, [EB] = 4×10^{-5} M, [Pb^{2+}] = 3 μM.

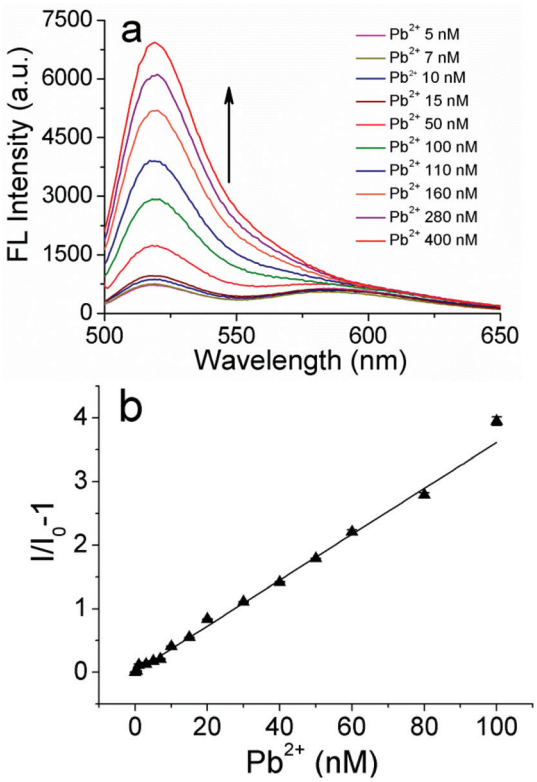

Fig. 2 (a) Fluorescence emission spectra of 17E/17S-FAM/EB in HEPES-Na (100 mM, pH 7.26) with the addition of aqueous of Pb^{2+}; (b) linear relationship between the increased ratio of fluorescence intensity and low Pb^{2+} concentrations. [17S-FAM] = 2×10^{-8} M, [17E] = 2×10^{-8} M, [EB] = 4×10^{-6} M. The error bars represent the standard deviations of three parallel measurements. The excitation wavelength is 490 nm.

(5 nM), Zhang *et al.*[31] (10 nM), Wu *et al.*[37] (1.5 nM), Fu *et al.*[38] (10 nM) Ali *et al.*[39] (20 nM) and by Chai *et al.*[40] (100 nM). Although some sensors reported lower LOD, such as 61.8 pM (reported by Wang *et al.*),[41] 200 pM (reported by Li *et al.*),[28] and 37 pM (reported by Zhuang *et al.*),[42] one of the sensors showed that the linear response of recovery rate was linearly dependent on the logarithm of the Pb^{2+} ion concentration,[41] and some of them required complicated and time-consuming procedures.[28,42] Obviously, our method is sensitive for the detection of Pb^{2+} ions and also is simple without any additional operation and washing procedures.

To optimize the hydrolysis time of DNAzyme, the fluorescence emission spectra of 17E-17S-FAM duplex/EB were measured after the 17E-17S-FAM duplex was incubated with lead ions for different times. In this case, different concentrations of Pb^{2+} from 10 nM to 400 nM are investigated, respectively. Firstly, the concentration of Pb^{2+} is fixed at 400 nM, which can ensure that the 17E-17S-FAM duplex is cleaved completely. As shown in Fig. 3, the intensity of FAM increases gradually with prolonging the incubation time. When the duplex is hydrolyzed for 20 min, the intensity of FAM reaches the highest value. Even when the solution is incubated for another 5 min, the intensity remains constant, which means that 20 min is enough for 17E-17S-FAM duplex hydrolysis by lead ions. Also, the increased intensity ratios reach the plateau at 20 min. Obviously, the same results were obtained at other concentrations of Pb^{2+}, such as 10 nM, 100 nM and 200 nM. As a result, the 20 min reaction time was selected for the analysis which demonstrates that this method is easy and rapid.

To estimate the selectivity of the new biosensor for Pb^{2+} analysis, we have challenged it against other metal ions including Mg^{2+}, Mn^{2+}, K^{+}, Ni^{2+}, Cd^{2+}, Ca^{2+}, Cu^{2+}, Hg^{2+}, Na^{+}, Zn^{2+}, Co^{2+} and their mixtures according to the same procedure. These metal ions were chosen because they all showed relatively high catalytic activity toward the cleavage. Fig. 4 shows

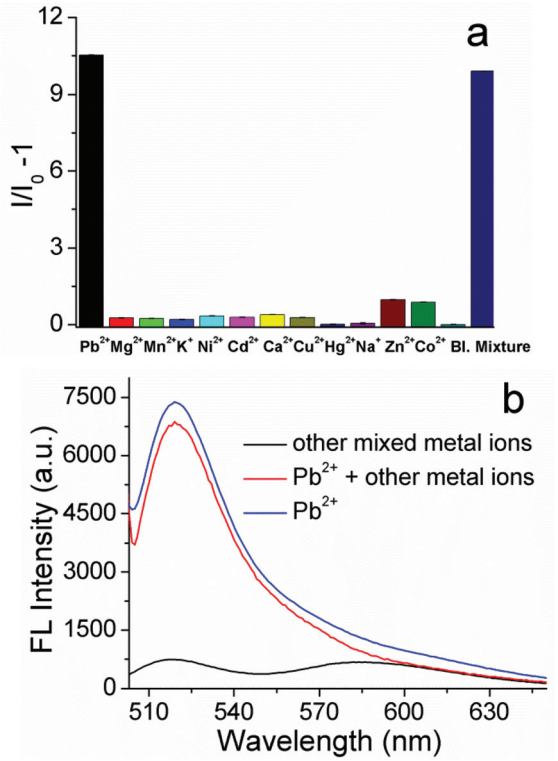

Fig. 4 (a) Selectivity of the proposed DNAzyme method toward Pb^{2+} ions; (b) fluorescence emission spectra of 17E-17S-FAM/EB in the Pb^{2+}, Pb^{2+}/other mixed metal ions, and other mixed metal ions, respectively. [17S-FAM] = 2×10^{-8} M, [17E] = 2×10^{-8} M, [EB] = 4×10^{-6} M, [Pb^{2+}] = 3×10^{-7} M. The concentration of each of the other metal ions was 3×10^{-7} M. The error bars represent the standard deviations of three parallel measurements. The excitation wavelength is 490 nm. The Bl. is the abbreviation of blank.

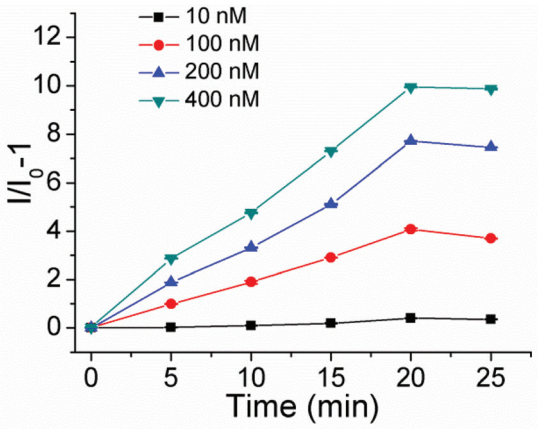

Fig. 3 Ratio of fluorescence at 520 nm as a function of ADA reaction time at different concentrations of Pb^{2+}. [17S-FAM] = 2×10^{-8} M, [17E] = 2×10^{-8} M, [EB] = 4×10^{-6} M. The error bars represent the standard deviations of three parallel measurements. The excitation wavelength is 490 nm.

that the intensity of FAM does not increase further in the presence of other metal ions except for Co^{2+} and Zn^{2+}. However, the increased ratios caused by Co^{2+} and Zn^{2+} are also pretty limited relative to target Pb^{2+}. Therefore, this assay presents a quite high selectivity for Pb^{2+}. In addition, to study the selectivity of this assay in the complicated system, other metal ions such as Mg^{2+}, Mn^{2+}, K^{+}, Ni^{2+}, Cd^{2+}, Ca^{2+}, Cu^{2+}, Hg^{2+}, Na^{+}, Zn^{2+}, and Co^{2+} were added into this biosensor system at the concentration of 300 nM, respectively. As shown in Fig. 4b, when other metal ions were added into the system, no obvious fluorescence enhancement of FAM could be observed in the absence of Pb^{2+}. Whereas when we added Pb^{2+} into the mixture solution, we can observe the great fluorescence enhancement at 520 nm from the fluorescence emission spectra, which means Pb^{2+} can excellently activate the DNAzyme to cleave the substrate even in the presence of other metal ions. These results reveal that the biosensor can serve as a novel fluorescence sensor for sensitive and selective Pb^{2+} detection.

In order to test the applicability of our method, the recovery experiments with spiked Pb^{2+} in river water samples were performed using the same experimental procedure. The results

are shown in Fig. S4.† River water was simply filtered to get rid of the insoluble materials and then it was diluted in the final assay mixture, and an aliquot of the standard Pb^{2+} content was added, respectively. Good recovery rates from 101.1% to 107.0% were obtained by using this method (Table S1†), and the CV for three repeated analyses of each sample is 1.3%–3.8%. Therefore, the experimental results demonstrate that our assay is applicable for the detection of lead ions in real samples with other potentially competing substances coexisting.

Conclusions

In conclusion, we have designed a simple, sensitive and selective method to detect Pb^{2+} by taking advantage of remarkable fluorescence turn-on in the presence of Pb^{2+}. The cleavage of the substrate by the 17E in the presence of Pb^{2+} causes its structure change from a 17E/17S-FAM duplex to ssDNA.[18] The FRET from 17E-17S-FAM to EB thus is broken, which leads to the fluorescence of FAM enhancing dramatically. The detection limit of Pb^{2+} is 530 pM, which is lower than most of the other methods reported in the literature. The method is simple, rapid and convenient, avoiding complicated procedures such as annealing and washing steps. Furthermore, this method provides a new platform for aptamer-based biosensors for the detection of other targets in aqueous solution.

Acknowledgements

The authors are grateful for the financial support from the National Natural Science Foundation of China (Grants 21222509), the 111 Project (Grant B14041), the Program for Changjiang Scholars and Innovative Research Team in University (IRT 14R33), and the Program for Innovative Research Team in Shaanxi Province (no. 2014KCT-28).

Notes and references

1 Y. Xiang, A. Tong and Y. Lu, *J. Am. Chem. Soc.*, 2009, **131**, 15352–15357.
2 S. Panich, K. A. Wilson, P. Nuttall, C. K. Wood, T. Albrecht and J. B. Edel, *Anal. Chem.*, 2014, **86**, 6299–6306.
3 H. Needleman, *Annu. Rev. Med.*, 2004, **55**, 209–222.
4 S. Wuertz, P. L. Bishop and P. A. Wilderer, *Biofilms in wastewater treatment: an interdisciplinary approach*, IWA, London, 2003.
5 M. Ochsenkuhn-Petropoulou and K. M. Ochsenkuhn, *Fresenius' J. Anal. Chem.*, 2001, **369**, 629–632.
6 J. E. Tahan, J. M. Sanchez, H. S. Cubillan and R. A. Romero, *Sci. Total Environ.*, 1994, **144**, 59–71.
7 J. Wu and E. A. Boyle, *Anal. Chem.*, 1997, **69**, 2464–2470.
8 H. N. Kim, W. X. Ren, J. S. Kim and J. Yoon, *Chem. Soc. Rev.*, 2012, **41**, 3210–3244.
9 X. B. Zhang, R. M. Kong and Y. Lu, *Annu. Rev. Anal. Chem.*, 2011, **4**, 105–128.
10 Y. Du, B. L. Li and E. K. Wang, *Acc. Chem. Res.*, 2013, **46**, 203–213.
11 D. Li, S. P. Song and C. H. Fan, *Acc. Chem. Res.*, 2010, **43**, 631–641.
12 E. M. Nolan and S. J. Lippard, *Chem. Rev.*, 2008, **108**, 3443–3480.
13 J. W. Liu, Z. H. Cao and Y. Lu, *Chem. Rev.*, 2009, **109**, 1948–1998.
14 M. Telting-Diaz and E. Bakker, *Anal. Chem.*, 2002, **74**, 5251–5256.
15 N. Nagraj, J. Liu, S. Sterling, J. Wu and Y. Lu, *Chem. Commun.*, 2009, 4103–4105.
16 C. W. Liu, C. C. Huang and H. T. Chang, *Anal. Chem.*, 2009, **81**, 2383–2387.
17 G. Zhu and C. Y. Zhang, *Analyst*, 2014, **139**, 6326–6342.
18 Y. Zhang, L. J. Wang and C. Y. Zhang, *Chem. Commun.*, 2014, **50**, 1909–1911.
19 C. S. Wu, M. K. Khaing Oo and X. Fan, *ACS Nano*, 2010, **4**, 5897–5904.
20 J. Liu and Y. Lu, *J. Am. Chem. Soc.*, 2004, **126**, 12298–12305.
21 J. Liu and Y. Lu, *J. Am. Chem. Soc.*, 2005, **127**, 12677–12683.
22 Z. D. Wang, J. H. Lee and Y. Lu, *Adv. Mater.*, 2008, **20**, 3263–3267.
23 D. Mazumdar, J. W. Liu, G. Lu, J. Z. Zhou and Y. Lu, *Chem. Commun.*, 2010, **46**, 1416–1418.
24 X. M. Miao, L. S. Ling and X. T. Shuai, *Chem. Commun.*, 2011, **47**, 4192–4194.
25 X. H. Zhao, R. M. Kong, X. B. Zhang, H. M. Meng, W. N. Liu, W. Tan, G. L. Shen and R. Q. Yu, *Anal. Chem.*, 2011, **83**, 5062–5066.
26 Y. Wen, C. Peng, D. Li, L. Zhuo, S. He, L. Wang, Q. Huang, Q. H. Xu and C. Fan, *Chem. Commun.*, 2011, **47**, 6278–6280.
27 P. J. J. Huang and J. W. Liu, *Anal. Chem.*, 2014, **86**, 5999–6005.
28 W. Y. Li, Y. Yang, J. Chen, Q. F. Zhang, Y. Wang, F. Y. Wang and C. Yu, *Biosens. Bioelectron.*, 2014, **53**, 245–249.
29 S. R. Tang, P. Tong, H. Li, J. Tang and L. Zhang, *Biosens. Bioelectron.*, 2013, **42**, 608–611.
30 H. Xu, P. P. Xu, S. M. Gao, S. X. Zhang, X. C. Zhao, C. H. Fan and X. L. Zuo, *Biosens. Bioelectron.*, 2013, **47**, 520–523.
31 L. Zhang, B. Han, T. Li and E. Wang, *Chem. Commun.*, 2011, **47**, 3099–3101.
32 S. Wang, B. S. Gaylord and G. C. Bazan, *J. Am. Chem. Soc.*, 2004, **126**, 5446–5451.
33 Q. H. Xu, S. Wang, D. Korystov, A. Mikhailovsky, G. C. Bazan, D. Moses and A. J. Heeger, *Proc. Natl. Acad. Sci. U. S. A.*, 2005, **102**, 530–535.
34 C. Wang, Y. L. Tang, Y. Liu and Y. Guo, *Anal. Chem.*, 2014, **86**, 6433–6438.
35 J. Liu and Y. Lu, *Anal. Chem.*, 2003, **75**, 6666–6672.
36 T. Li, S. J. Dong and E. K. Wang, *J. Am. Chem. Soc.*, 2010, **132**, 13156–13157.

37 Y. S. Wu, F. F. Huang and Y. W. Lin, *ACS Appl. Mater. Interfaces*, 2013, **5**, 1503–1509.
38 X. Fu, T. Lou, Z. Chen, M. Lin, W. Feng and L. Chen, *ACS Appl. Mater. Interfaces*, 2012, **4**, 1080–1086.
39 E. M. Ali, Y. G. Zheng, H. H. Yu and J. Y. Ying, *Anal. Chem.*, 2007, **79**, 9452–9458.
40 F. Chai, C. A. Wang, T. T. Wang, L. Li and Z. M. Su, *ACS Appl. Mater. Interfaces*, 2010, **2**, 1466–1470.
41 L. Wang, Y. Jin, J. Deng and G. Chen, *Analyst*, 2011, **136**, 5169–5174.
42 J. Zhuang, L. Fu, M. Xu, Q. Zhou, G. Chen and D. Tang, *Biosens. Bioelectron.*, 2013, **45**, 52–57.